scientific reports

Check for updates

OPEN

Discovery and functional characterization of canine PD-L1-targeted antibodies for evaluating antitumor efficacy in a canine osteosarcoma xenograft model

Min-young Song[1,4,6], Jaewon Cho[1,6], Hyosung Park[1], Yujeong Song[1], Keon Kim[2], Jae-Hee Ahn[1], Chang-Min Lee[2], Dae Hee Kim[1,3,5]✉ & Hyun-Jeong Ko[1,3,4,5]✉

Targeting the programmed cell death protein 1 (PD-1)/programmed death ligand 1 (PD-L1) pathway is promising in treating cancer in humans and offers potential for veterinary applications. However, no PD-L1 antibodies have been approved specifically for treating canine cancer. We aimed to develop PD-L1-specific antibodies using phage display technology for treating canine cancer. A synthetic antibody library was screened, and 18 high-affinity single-chain variable fragment clones were subsequently converted to the IgG format for enhancing binding affinity and functional stability. The clone #15 exhibited the highest binding affinity and most pronounced antitumor effects. The PD-1/PD-L1 interaction was inhibited by antibody #15. The binding and thermal stabilities of the antibodies were validated by flow cytometry and thermal stability assays, respectively. In NOG mice xenografted with canine osteosarcoma cells and treated with canine peripheral blood mononuclear cells and antibody #15, the tumor size and weight were reduced. Antibody #15 significantly increased apoptosis of tumor cells and lymphocyte populations. Therefore, anti-PD-L1 antibodies, particularly antibody #15, have substantial potential as novel immunotherapeutic agents against canine osteosarcoma. This study represents a significant advancement in veterinary oncology, with the potential of improving treatment outcomes for canine cancers and providing insights into similar strategies in human cancer therapy.

Keywords Canine cancer, Programmed death ligand 1, Immunotherapeutics, Antibody, Phage display

Cancer is a prevalent health concern in dogs, exhibiting various types depending on factors such as breed and sex[1–4]. In canine oncology, the incidence of cancer exceeds four million new cases annually, thereby making it a leading cause of disease-related mortality in dogs[5]. Common tumors in dogs include lymphoma, osteosarcoma, mast cell tumors, nasal tumors, and mammary cancer[6,7]. The traditional therapies for canine cancer include surgery, radiotherapy, and chemotherapy. Recently, the demand for effective cancer treatments for pets has increased, prompting the exploration of immunotherapeutic approaches in veterinary medicine[8].

Monoclonal antibodies are significantly used as immunotherapeutic agents for treating human cancers[9,10]. Monoclonal antibodies that specifically target immune checkpoint molecules and inhibit their signaling pathways have garnered significant attention, reflecting their potential in treating human cancers and promising potential use in canine cancers[11,12]. In particular, monoclonal antibodies targeting the programmed cell death protein 1 (PD-1)/programmed death ligand 1 (PD-L1) pathway have shown significant promise[13,14]. PD-L1 possesses

[1]Department of Pharmacy, Kangwon National University, Chuncheon 24341, Republic of Korea. [2]Department of Veterinary Internal Medicine, College of Veterinary Medicine and BK21 FOUR Program, Chonnam National University, Gwangju 61186, Republic of Korea. [3]Kangwon Institute of Inclusive Technology, Kangwon National University, Chuncheon 24341, Republic of Korea. [4]Innovative Drug Development Research Team for Intractable Diseases (BK21 Plus), Kangwon National University, Chuncheon 24341, Republic of Korea. [5]Global/Gangwon Innovative Biologics-Regional Leading Research Center (GIB-RLRC), Kangwon National University, Chuncheon 24341, Republic of Korea. [6]Min-young Song and Jaewon Cho have contributed equally to this work. ✉email: kimdh@kangwon.ac.kr; hjko@kangwon.ac.kr

distinctive structural features, including two Ig-like domains in the extracellular region, a transmembrane domain, and a short cytoplasmic domain without recognized signaling motifs[15]. It mediates immune protection against cytotoxic T lymphocytes and modulates chronic immune responses, with its upregulation disrupting immune-protective pathways[16]. PD-L1 plays a critical role in immune modulation by binding to PD-1 receptors on T-cells, leading to T-cell inactivation and allowing tumor growth. Manipulating the PD-1/PD-L1 pathway with monoclonal antibodies shows promise for boosting the activity of tumor-specific T-lymphocytes, resulting in an antitumor effect[17]. Alterations in immune checkpoint function significantly suppress the activity of tumor-specific T-lymphocytes[18,19].

Several studies have reported the presence of PD-L1 in canine tumors[20] and blocking PD-1/PD-L1 interaction has been shown to enhance T-cell function in dogs with cancer[21,22]. A monoclonal antibody specific for canine PD-L1 has demonstrated efficacy in treating oral melanoma[23]. Anti-PD-L1 antibodies have been developed to evaluate expression in other contexts[20]. Furthermore, elevated PD-L1 expression has been observed in canine osteosarcoma, suggesting that targeting this pathway may be beneficial[20]. Despite these promising findings, no PD-L1 antibodies have been approved specifically for treating canine cancer, thereby highlighting a significant gap in veterinary oncology.

To address this gap, we used phage display screening for developing antibodies suitable for immunotherapy. Through panning using a synthetic antibody library, we aimed to identify distinct single-chain variable fragment (scFv) clones against canine PD-L1. Subsequently, the selected scFv was ligated to the constant region of human IgG, resulting in the development of IgG-format antibodies with binding capabilities. We characterized their binding affinities and efficacies in vitro. A mouse model was established for evaluating the efficacies of canine anti-PD-L1 antibodies in vivo.

Methods

Cell lines and transfection

The canine osteosarcoma cancer cell line D17 was purchased from American Type Culture Collection, (ATCC; Manassas, VA, USA) and cultured in Dulbecco's Modified Eagle Medium with 4.5 g/L glucose, L-glutamine, and sodium pyruvate (Corning, NY, USA), supplemented with 10% (v/v) fetal bovine serum (FBS) (Gibco, Grand Island, NY, USA) and 1% (v/v) antibiotic–antimycotic solution (Welgene, Republic of Korea). HEK-293F cells were cultured in FreeStyle 293 Expression Medium (Gibco). FreeStyle 293-F cells (Gibco) were transfected using FectoPRO transfection reagent (Polyplus, Graffenstaden, France).

Animals

The animal experiments were conducted according to the guidelines of the Institutional Animal Care and Use Committee of Kangwon National University, Chuncheon, Republic of Korea (approval number: KW-230117-1) and Institutional Animal Care and Use Committee of Chonnam National University, Gwangju, Republic of Korea (approval number: CNU IACUC-YB-2023-101). Five-week-old female NOG (NOD.Cg-prkdc^{scid}IL2γg$^{tm1\ Sug}$/JicKoat) mice, deficient in T-, B-, and natural killer cells, were purchased from KOATECH (Pyeontaek, Republic of Korea). Mice were maintained in a specific pathogen-free facility on an 11-h light/13-h dark cycle.

Phage display panning

To conduct phage display panning for antibody screening, we used a synthetic antibody library (kindly provided by Prof. Hyunbo Shim, Ewha Womans University) for obtaining canine antibody clones that can bind to canine PD-L1. Recombinant Canine PD-L1/B7-H1 (ECD, hFc Tag) was purchased from SinoBiological (70110-D02H; Beijing, China). The antibody library had a diversity of 7.6×10^9, with scFvs tagged with HA at their C-terminus. The scFvs were reamplified as scFv-displaying phages, and phages from each round of panning were amplified using ER2738 cells (New England Biolabs, Ipswich, MA, USA). Library reamplification and phage display panning were performed following the protocols described in "Phage Display: A Laboratory Manual"[25]. For panning, scFv-displaying phages were inoculated into Luria–Bertani broth (LB) medium (BD Biosciences, San Jose, CA, USA) and then spread on LB Agar Miller (BD Biosciences) plates containing 1% D-glucose (Duchefa Biochemie, Haarlem, the Netherlands) and 100 μg/mL carbenicillin (GoldBio, St. Louis, MO, USA). After overnight culture, resuspended cells from colonies were inoculated into SB medium containing 1% w/v MOPS (Thermo Fisher Scientific, Waltham, MA, USA), 2% w/v Oxoid Yeast Extract (Thermo Fisher Scientific), and 3% Oxoid Tryptone (Thermo Fisher Scientific), and cultured at 37 °C for 2 h. Following this, VCSM13 helper phage (Stratagene, La Jolla, San Diego, CA, USA) at approximately 10^{12} colony-forming units (CFUs) was added to the cells, which were then transferred to fresh SB medium. After incubation at 37 °C and shaking at 210 rpm for 2 h, an equal volume of fresh medium containing 100 μg/mL carbenicillin and 70 μg/mL kanamycin (Duchefa Biochemie) was added. Following overnight culture, phages were precipitated using 5% w/v polyethylene glycol 8000 (Sigma-Aldrich, St. Louis, MO, USA) and 0.5 M NaCl (Avantor, PA, USA)). Panning for the enrichment of binders was conducted using immunotubes (Thermo Fisher Scientific) coated with canine PD-L1 (SinoBiological). To block nonspecific binders, a blocking solution of phosphate-buffered saline (PBS; iNtRON Biotechnology, Republic of Korea) containing 0.1% Tween 20 (PBST) and 5% (w/v) skim milk (BD Biosciences) or 5% (w/v) bovine serum albumin (BSA; HanLAB, Republic of Korea) was applied to the immunotube for 1 h at room temperature. The immunotube was then incubated with the purified phages for 2 h at room temperature. To ensure precision and high-affinity binding, the immunotube was washed once for the first panning round, twice for the second panning round, and thrice for the third and fourth panning rounds using 0.1% PBST. Phages bound to canine PD-L1 were eluted with 0.25% trypsin (Gibco) and used to infect ER2738 cells for amplification. Phage-infected cells were rescued. Four rounds of panning were performed to enrich the scFv binders, and colonies were randomly picked after the third and fourth rounds of panning for subsequent binding assays.

scFv expression and periplasmic extraction

Single colonies expressing individual scFvs from the third and fourth panning rounds were randomly picked and grown overnight at 37 °C with shaking at 210 rpm in a deep-96-well plate containing 1 mL/well LB medium with 100 μg/mL carbenicillin. The next day, 20 μL overnight culture was inoculated into 800 μL/well LB medium containing 100 μg/mL carbenicillin and cultured at 37 °C with shaking at 210 rpm for 2 h. After 2 h, 200 μL of 5 mM isopropyl β-d-1-thiogalactopyranoside (Duchefa Biochemie) was added to each well, and the cultures were grown overnight at 30 °C with shaking at 210 rpm. Crude periplasmic extracts containing scFvs were extracted using the osmotic shock method. The cultures grown overnight were centrifuged at 3,500 rpm for 20 min at room temperature to remove the culture medium. After discarding the supernatant, the pellet was resuspended in ice prechilled 1X TES buffer and incubated on ice for 30 min. Next, 0.2X TES buffer was added to each well and incubated on ice for 30 min. Finally, the resuspended samples were centrifuged at 3,500 rpm for 20 min at 4 °C. And then, supernatants containing periplasmic crude extracts were used in the experiments. For thermal stability assay, periplasmic crude extracts were incubated at 70 °C for 10 min and then on ice for 30 min. ELISA was performed with the supernatants after this processing.

Expression of IgG-format antibodies with a two-vector system of heavy and light chains and their purification

Eighteen scFvs having independent sequence information were analyzed and found to have a VH domain–Linker–VL domain structure. Primers for this structure were synthesized and used to amplify individual heavy and light variable fragments using a KAPA HiFi HotStart PCR Kit (Roche Sequencing, Indianapolis, IN, USA). The VH primer was designed with restriction sites for BamHI at the 5' end and NheI at the 3' end, while the VL primer was designed with restriction sites for BamHI at the 5' end and BsiWI at the 3' end. After amplification of the VH and VL domains by polymerase chain reaction (PCR), the PCR products of each clone were ligated into a pCEP4 mammalian cell expression vector (Invitrogen, Carlsbad, CA, USA). The vector, along with the VH and VL fragments, was fused with CH1-hinge-CH2-CH3 for expression of the heavy chain or Cκ for expression of the light chain. Each clone of the heavy and light chain vectors was properly combined and co-transfected into FreeStyle 293-F cells at a 2:1 ratio (light) of DNA and FectoPRO transfection reagent, according to the manufacturer's protocol. After 9 days, the culture medium was harvested, and the IgG-format clones were purified by open-column chromatography using protein A agarose beads (Repligen, Waltham, MA, USA). After purification and dialysis with PBS at pH 7.5, antibody concentration was spectrophotometrically quantified, and purity of the antibodies was assessed by sodium dodecyl sulfate–polyacrylamide gel electrophoresis (SDS–PAGE) and Coomassie Brilliant Blue staining (Biosesang, Republic of Korea).

Binding assay with direct ELISA

The binding activities of individual scFv and IgG were assessed by ELISA. For the binding assay, 500 ng/mL canine PD-L1-hFc in PBS was coated onto a 96-well ELISA plate and incubated at 4 °C overnight. After discarding the solution, each well was blocked with 3% (w/v) skim milk in 0.1% PBST and incubated for 1 h at 37 °C. Then, 100 μL scFv-containing periplasmic crude extract or 200 ng purified IgG was added to each well and incubated for 2 h at room temperature. Plates were washed with tap water, and horseradish peroxidase (HRP)-conjugated anti-HA (1:5000; Roche, Basel, Switzerland) or HRP conjugated anti-human Fc (1:5000; Jackson ImmunoResearch, West Grove, PA, USA) in blocking buffer was added and incubated for 45 min at 37 °C. For detection, 50 μL of 3,3',5,5'-tetramethylbenzidine substrate (BD Biosciences) was added to each well, and the absorbance was measured at 450 nm using a BioTek Epoch microplate reader (Agilent, Santa Clara, CA, USA).

Inhibition assay with direct ELISA

The inhibitory activities of individual scFv and IgG were assessed by ELISA. For the inhibition assay, cross-species interaction of human PD-1 and canine PD-L1 was used and either human PD-1 or caninePD-L1 were immobilized on the ELISA plates and the bindings of respective PD-L1 or PD-1 were assessed in co-incubation condition with anti-caninePD-L1 scFvs. 500 ng of either canine PD-L1-mFc or human PD-1- human Cκ in PBS was coated onto each well of a 96-well ELISA plate and incubated at 4 °C overnight. After discarding the solution, each well was blocked with 3% (w/v) skim milk in 0.1% PBST and incubated for 1 h at 37 °C. Then, 100 μL scFv-containing periplasmic crude extract was mixed respectively with 100 ng human Cκ-conjugated human PD-1 or mouse Fc-conjugated canine PD-L1, then added to each well and incubated for 2 h at room temperature, followed by washing with tap water. HRP-conjugated anti-human Cκ (1:5000; Jackson ImmunoResearch, West Grove, PA, USA) for detection of PD-1 binding or HRP-conjugated anti-mouse Fc (1:5000; Jackson ImmunoResearch, West Grove, PA, USA) for the detection of PD-L1 was incubated in blocking buffer for 45 min at 37 °C. For detection, 50 μL of 3,3',5,5'-tetramethylbenzidine substrate (BD Biosciences) was added to each well, and the absorbance was measured at 450 nm using a BioTek Epoch microplate reader (Agilent, Santa Clara, CA, USA). The inhibition efficacy (%) for each scFv, normalized by the positive control, was calculated as follows:

$$\text{Inhibition efficacy } (\%) = 100 - ((\text{OD}_{\text{test scFv}}/\text{OD}_{\text{positive control}}) \times 100\%)$$

Flow cytometry

To analyze the specific binding of purified IgG to cell-surface canine PD-L1, we used a BD FACSVerse flow cytometer (BD Biosciences). In each experiment, 1×10^5 D17 cells were used. Cells were resuspended using Cell Dissociation Buffer Enzyme-Free PBS-based (Gibco) and washed with FACS buffer containing TBS (iNtRON), 0.5% BSA (HanLAB), and 0.05% NaN_3 (Acros Organics, Geel, Belgium). Cells were then resuspended in FACS buffer and incubated with 25 μg/mL purified IgG at 4 °C for 1 h. After washing with FACS buffer, Alexa Fluor 488-conjugated anti-human Fc (1:500; Jackson ImmunoResearch) or Alexa Fluor 647-conjugated anti-human Fc

(1:500; Jackson ImmunoResearch) was added to each IgG clone and incubated at 4 °C for 1 h. Finally, all samples were assessed using a FACSVerse flow cytometer and analyzed using FlowJo software (FlowJo LLC, Ashland, OR, USA).

Canine PD-1/PD-L1 blockade bioassay

To determine whether the antibody effectively blocks the interaction between cells expressing canine PD-1 and those expressing PD-L1, we used a canine PD-1/PD-L1 blockade bioassay (Promega, Madison, WI, USA). The inhibitory activity of antibodies was assessed using an NFAT-mediated luciferase reporter assay. Canine PD-L1 aAPC/CHOK1 cells (100 µL/well) were seeded into white flat-bottom 96-well plates in prewarmed F12 medium containing 10% FBS and incubated for 17 h at 37 °C under 5% CO_2. Then 95 µL F12 medium was removed from each well. Samples were diluted in assay buffer (prewarmed RPMI1640 containing 1% FBS) and, 40 µL was poured in each well. The antibodies were applied at 9 different concentrations, starting at 100 nM. The second concentration was a two-fold diluted to 50 nM, followed by seven additional concentrations obtained through three-fold serial dilutions.

Canine PD-1 effector cells were suspended in the assay buffer and seeded at 40 µL/well. Cells were co-incubated at 37 °C for 4 h. Then 80 µL Bio-Glo reagent was added and incubated for 10 min at room temperature.

All solutions were provided by the canine PD-1/PD-L1 blockade bioassay kit. Luminescence of the antibody samples was measured using a microtiter plate reader VICTOR X4 (Perkin Elmer, Waltham, MA, USA).

In vivo animal experiment

After the stabilization period, 6-week-old NOG mice were subcutaneously xenografted onto the left flank with 4×10^6 D17 cells[24]. Tumor volumes were calculated as the product of $XY^2/2$ (X, long axis; Y, Short axis). When the tumor volumes reached approximately 30 mm^3, 2×10^6 canine peripheral blood mononuclear cells (PBMCs) were injected into tumor-bearing mice via the tail vein. Canine PD-L1 antibodies were injected intraperitoneally at a dose of 5 mg/kg (1 mg/mL) on the 10th day after tumor transplantation. Tumor volumes were measured every 2 days. All mice were euthanized by CO_2 inhalation. After euthanized mice groups, tumor was obtained from mice and measured weight. The obtained cancer tissues were stored in 4% paraformaldehyde.

Ethics statement

All experiments were performed in the principles of the ARRIVE guidelines. All animal studies were performed and approved in accordance with the relevant guidelines by the Institutional Animal Care and Use Committee of Kangwon National University.

Results

Discovery of antibodies that specifically binds to canine PD-L1

To isolate antibody clones that bind to the extracellular domain of canine PD-L1, scFvs that bind to canine PD-L1 were screened using phage display technology[26]. A synthetic scFv library with a diversity of 7.6×10^9 was used (Fig. 1A). A total of 192 random scFv clones from the third and fourth panning output pools were cultured, and their periplasmic extracts were harvested and used for primary binding assays. To assess the number of independent scFv antibodies, ELISA test was performed first and the sequences of positive clones were sequence-analyzed. Owing to the complexity of contents in the periplasmic fraction and difficulties of normalizing the expression of individual clones, primary antibody assays were performed qualitatively. After the 4th panning, the infection titer measured using ER2739 cells increased (3.5×10^9 CFU) as compared with the titer after the 3rd panning (4.3×10^7 CFU), suggesting that the panning pool of scFv, which binds to canine PD-L1, was abundant. Enrichment of antibody binders was demonstrated by an apparent increase in phage recovery (output phages/input phages) in the 4th round of panning (Fig. 1B). ELISA confirmed high binding affinities of the selected scFv clones for canine PD-L1. A total of 35 scFv clones that exhibited meaningful binding signals for canine PD-L1 (absorbance at 450 nm exceeding 0.2) were identified and are marked with a red arrow (Fig. 1C). DNA sequences from phage-infected cells were analyzed for the 35 candidates, resulting in the identification of 18 clones with distinct sequences in the complementarily determining regions. To explore the feasibility of using the canine PD-L1 antibody as a therapeutic drug, we assessed the thermal stability of the selected 18 clones through heat treatment at 70 °C, inducing conformational changes, followed by lowering the temperature to allow structural reform. ELISA results demonstrated thermal stability of the scFv clones as they maintained binding efficacy with canine PD-L1 even after heating (Fig. 1D). In summary, a diverse scFv library was screened using phage display technique, yielding 18 distinct high-affinity and thermostable scFv clones that specifically bind to canine PD-L1.

Screening of functional scFvs

To verify the inhibitory efficacies of the antibody clones, human PD-L1 was used as a competitive binder in competitive ELISA. Despite 76.04% sequence homology between canine PD-L1, identical sequences were observed, which are outlined in the black box (Supplementary Fig. 1A). Notably, the regions highlighted in yellow denote essential binding sites for human PD-1, suggesting similarities in the binding sites between canine and human PD-L1[27] (Supplementary Fig. 1B). Based on the high degree of conservation observed in the crucial binding regions between canine and human PD-L1, we expected that the scFvs would also bind to human PD-L1 and compete with canine PD-L1 and human PD-1 binding. Consequently, we utilized human PD-1 in the competitive ELISA assay instead of canine PD-1. We noticed that certain scFvs bound to human PD-L1 (Fig. 2A and B). We validated the functionality of scFvs by assuming that the desired antibodies would bind to PD-L1 in a manner similar to that of human PD-1.

We quantified the effectiveness of canine scFvs in impeding the interaction between canine PD-L1 and human PD-1 (Fig. 2A and B). Upon analyzing the results of competitive ELISA, a notable decrease in absorbance

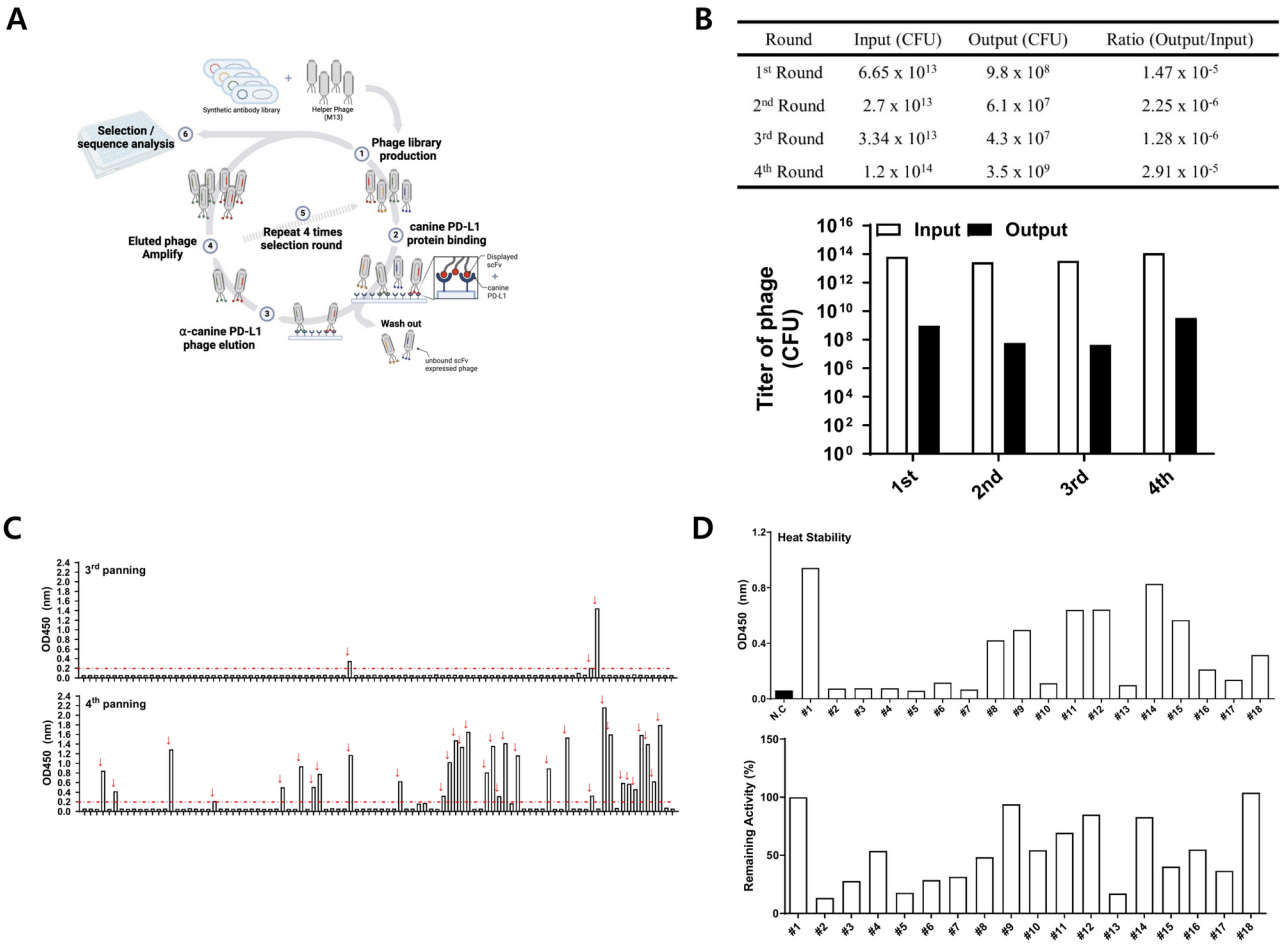

Round	Input (CFU)	Output (CFU)	Ratio (Output/Input)
1st Round	6.65×10^{13}	9.8×10^{8}	1.47×10^{-5}
2nd Round	2.7×10^{13}	6.1×10^{7}	2.25×10^{-6}
3rd Round	3.34×10^{13}	4.3×10^{7}	1.28×10^{-6}
4th Round	1.2×10^{14}	3.5×10^{9}	2.91×10^{-5}

Fig. 1. Screening of canine anti-PD-L1 antibodies and generation of scFv clones. (**A**) Schematic of phage display. (**B**) Titration for panning was repeated four times. Titer was determined based on the number of phage-infected ER2738 colonies. (**C**) Binding assay of scFvs by ELISA for selecting specific binders to canine PD-L1. (**D**) The heat stability of 18 scFv clones analysed by a binding assay.

was observed upon the introduction of canine scFvs, compared to those of samples treated solely with canine PD-L1 and human PD-1. This observation strongly indicated an effective inhibition of binding between canine PD-L1 and human PD-1 by the scFvs (Fig. 2C and D). After assessing the binding affinity with canine PD-L1, thermal stability, and PD-1/PD-L1-blocking activity of each scFv, those exhibiting relatively high binding affinity to canine PD-L1 were selected and engineered for conversion into the IgG format.

Functional verification of canine PD-L1-specific scFv-derived IgGs

We cloned five top-priority scFvs, including #1, #8, #11, #14, and #15, into the IgG form. VH and VL sequences were cloned and inserted into expression vectors capable of producing human IgG (Supplementary Fig. 2A). The assembly of the expressed IgGs with disulfide bonds consisting of two heavy and two light chains was confirmed using SDS–PAGE under both reducing and nonreducing conditions. The protein bands observed in all five samples indicated the presence of intact IgG (Fig. 3A, Supplementary 2C). We observed that the binding affinities of the expressed IgGs for canine PD-L1 remained consistent (Fig. 3B). Clones #8 and #15 exhibited strong binding signals, whereas clones #1, #11, and #14 did not show significant binding with D17 cells (Fig. 3C, Supplementary Fig. 2B). In summary, we validated that the IgGs derived from scFvs displayed substantial functional binding to canine PD-L1 and ultimately selected two clones, #8 and #15, for further analysis.

Efficacy of canine PD-L1-specific antibodies

To investigate the efficacy of the canine PD-L1-specific antibodies, a mixed lymphoid reaction was performed. Mixed lymphoid reaction is an in vitro assay, in which immune cells from two canine species are cocultured to trigger "non-self" recognition required for immune checkpoint regulation. Five canine PD-L1-specific IgGs were co-cultured with two different canine PBMCs (5×10^4 cells). Every candidate of antibodies was treated with 0, 5, 10 and 20 μg/mL and incubated for 3 days and measured the proliferation by Cell Counting Kit 8. As previously observed, clones #8 and #15 showed significantly upregulated proliferation depending on the antibody concentration (Fig. 4A). Based on their binding affinities and sequence specificities, we selected two antibodies, #8 and #15, for further analysis. We compared the antibodies #8 and #15 with atezolizumab that

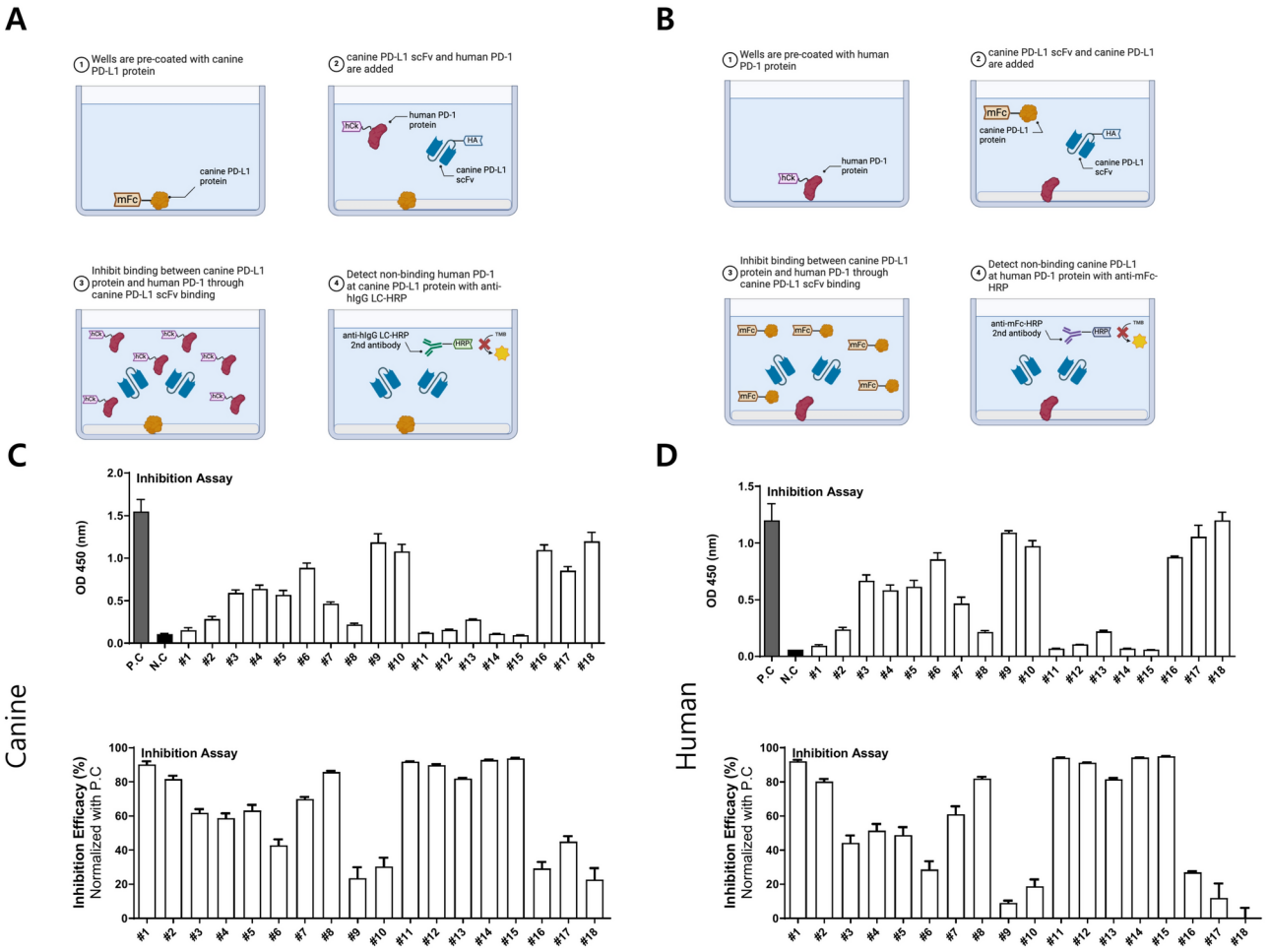

Fig. 2. Development of an in vitro PD-1/PD-L1 interaction inhibition assay and validation of functional activities of scFvs. (**A, B**) Schematic for verifying inhibition of the binding between human PD-1 and canine PD-L1 by 18 scFvs using competitive ELISA. (**C**) Data of the competitive ELISA. In the graph, P.C is the control treated only with canine PD-L1 (tag: mouse Fc) and human PD-1 (tag: human Cκ), whereas N.C is the control where only canine PD-L1 was used, followed by treatment with secondary antibody. (**D**) The scFv candidates were treated simultaneously with canine PD-L1 protein, and the residual levels of canine PD-L1 were determined using α-mouse Fc-HRP. The results were measured at OD 450 nm.

binds canine PD-L1. The half maximal effective concentration (EC_{50}) values for atezolizumab, #8, and #15 were 1.9187, 6.2633, and 0.74452 μg/mL, respectively (Fig. 4B). A comparison of the EC_{50} values indicated that antibody #15 could induce a response and an equal effect at a lower concentration than did atezolizumab. This suggests that antibody #15 demonstrated superior efficacy than did the other antibodies.

Antitumor effect of the selected antibodies against canine osteosarcoma cancer

In this study, we developed new candidate anti-PD-L1 antibodies that can bind with both canine and human PD-L1. As our studies confirmed the affinity against canine PD-L1 in vitro, we investigated its effectiveness in vivo (Fig. 5A). NOG mice administered PBMCs in combination with antibodies #8 and #15 demonstrated a reduction in tumor size compared to that of the control group, which received only PBMCs (Fig. 5B). The group with antibody #15 showed the lowest tumor volume and least tumor growth compared to those of the other groups (Fig. 5C). To assess the anti-tumor effects were mediated with canine anti-PD-L1 antibodies, TUNEL assay were proceeded. The control group, which received only PBMC, exhibited minimal migration of canine T cells and a low number of TUNEL-positive apoptotic cells. In contrast, the groups treated with antibodies #8 and #15 following PBMC transfer showed increased T cell infiltration and a higher number of apoptotic cells within the tumor. Moreover, canine #15 antibody significantly upregulated apoptosis of tumor cells and the lymphocyte population (Fig. 5D). These results suggest that canine #15 antibody could be a novel antitumor immunotherapy for dogs.

Discussion

Cancer in dogs shares numerous characteristics with human cancers, including histological appearance, tumor genetics, molecular targets, biological behavior, and response to conventional therapies[28,29]. Tumor

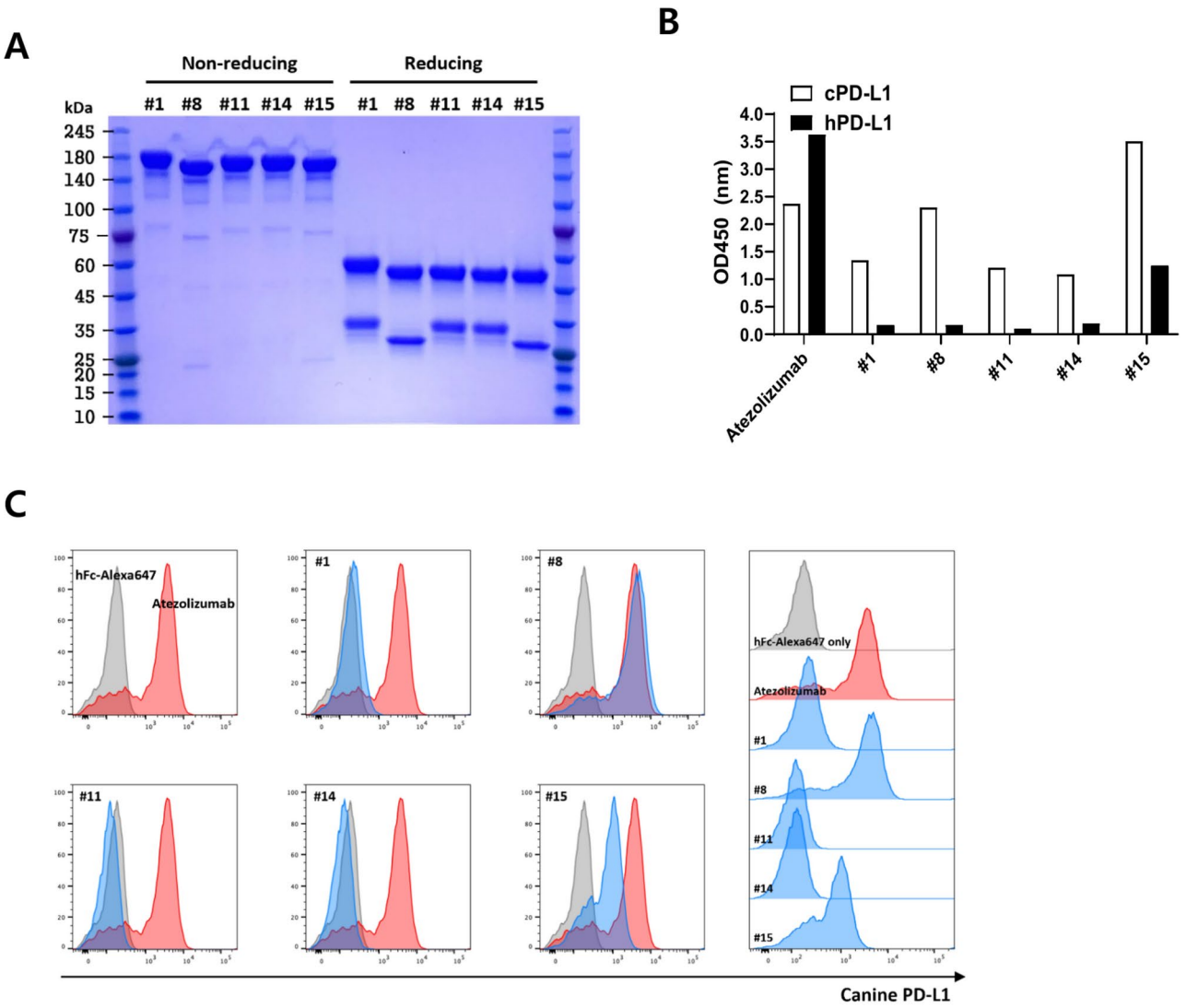

Fig. 3. Conversion to IgG form of selected scFv and function verification. Coomassie blue-stained gel images of purified IgGs. (**B**) Binding affinity of canine anti-PD-L1 antibodies against canine and human PD-L1 through ELISA. Atezolizumab was used as a positive control. (**C**) Binding of five canine anti-PD-L1 antibodies with canine cell lines expressing PD-L1 measured by flow cytometry. [Atezolizumab (red line), canine anti-PD-L1 antibodies (blue line), and control antibody (black line)].

initiation and progression are influenced by similar factors, such as age, nutrition, sex, reproductive status, and environmental exposure[30]. However, the treatment modalities for canine tumors are currently restricted to surgery, chemotherapy, and radiotherapy[31]. These conventional therapeutic approaches present several limitations, including collateral damage to non-cancerous cells and a lack of efficacy in certain subjects with tumors. Additionally, these treatments are associated with various adverse effects such as vomiting, loss of appetite, fatigue, skin damage, and drug resistance. Moreover, certain cancers require the concurrent use of multiple treatment modalities[32,33].

As interest in treating tumors in companion animals has increased, recent studies have demonstrated the beneficiary potential of antibodies targeting immune checkpoint molecules in treating canine cancer[34,35]. In particular, studies on canine anti-cytotoxic T-lymphocyte-associated antigen 4 (CTLA-4) antibody is currently in progress[36], and additional studies include the development and clinical trials of canine anti-PD-L1 and anti-PD-1 antibodies[20,23,37]. Blocking the PD-L1/PD-1 pathway with canine anti-PD-L1 antibody increases the production of interferon gamma in tumor-infiltrating cells in dogs[21]. We noticed the necessity of identifying sequence homology of amino acids between human and canine species for target molecules currently under investigation and those that are potential investigational targets. PD-L1, CTLA-4, and C–C motif chemokine receptor 4 exhibit approximately 86%, 85%, and 90% sequence homology between humans and dogs, respectively[21]. Dogs can naturally develop various types of cancers like human tumors, and genetic and epigenetic features between canine and human cancers overlap more than those in mouse models[38,39]. Specifically, pathological and molecular similarities in breast cancer, shared molecular targets, like epidermal growth factor receptor (EGFR)

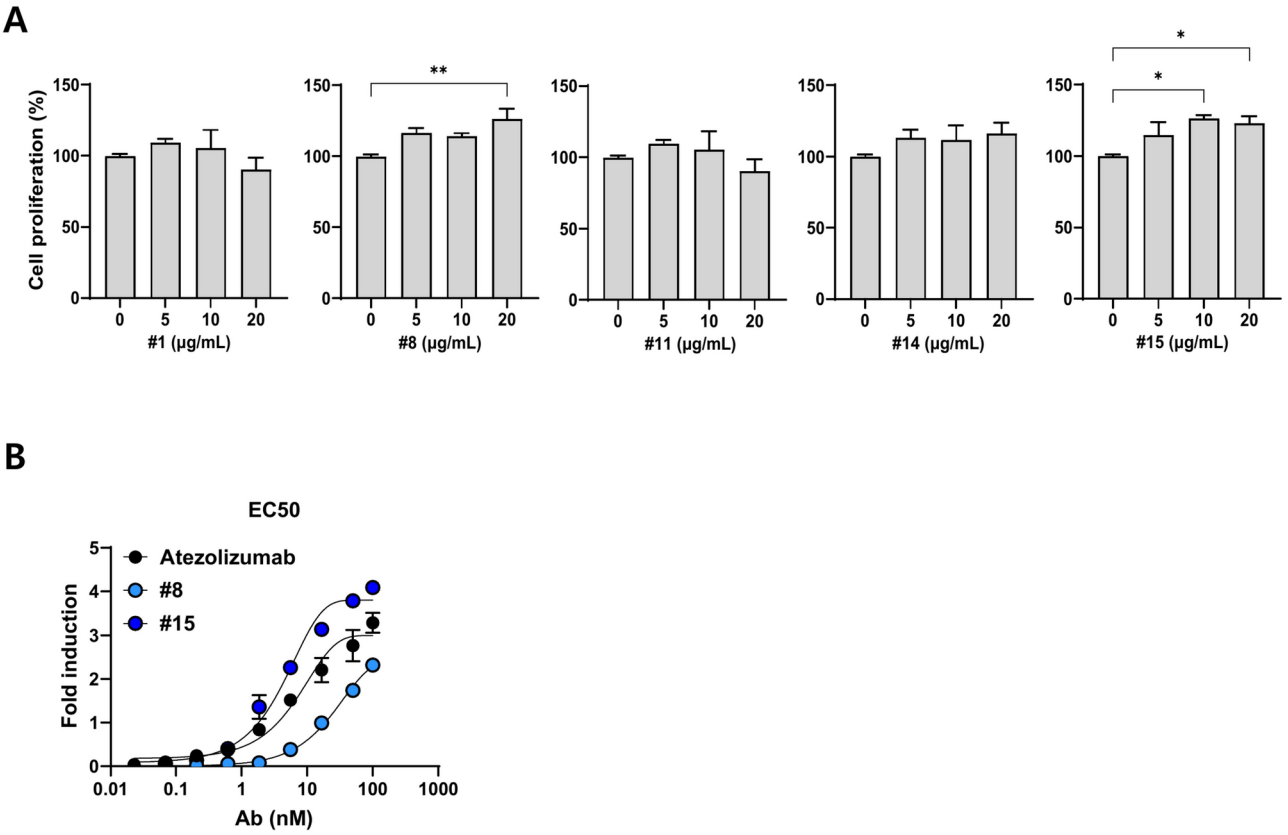

Fig. 4. Inhibitory efficacy of canine anti-PD-L1 antibody candidates against canine PD-L1 in vitro. (**A**) Canine PD-L1-specific IgG candidates were co-cultured with two different sets of 5×10^4 canine PBMCs. Each candidate was treated with 0, 5, 10, and 20 μg/ml, incubated for 3 days, and the proliferation was measured using CCK8. (**B**) The inhibitory efficacy of canine anti-PD-L1 antibodies validated through a Canine PD-1/PD-L1 Blockade Bioassay.

and human epidermal growth factor receptor 2, in bladder cancer, and similar profiles of diffuse large B-cell lymphoma between humans and dogs have been reported[5,40,41]

Our study focused on addressing the significant gap in veterinary oncology by developing new candidates for anti-PD-L1 antibodies, which can bind to both canine and human PD-L1. The results of this study are promising for several reasons. First, phage display technology allowed us to efficiently screen and identify high-affinity antibody candidates from a vast library. This approach can also be applied to other targets in veterinary medicine, potentially accelerating the development of novel therapeutics. Second, the conversion of scFvs to the IgG format enhanced the binding affinity and ensured that the antibodies retained their functional integrity when tested in a physiological context. Furthermore, an efficacy evaluation using a xenograft model confirmed the significant antitumor effects of the antibodies, particularly #15, in a relevant biological setting. This antibody demonstrated the highest binding affinity and most significant antitumor effect in our in vivo experiments. The ability of #15 to promote lymphocyte infiltration and induce apoptosis in tumor cells suggests that it effectively reactivates the immune response against cancer cells. These results highlight the potential of #15 as a lead candidate for further development and clinical testing in dogs with osteosarcoma, and possibly in other cancers that express PD-L1. Additionally, changing the human Fc sequence to a canine Fc sequence may increase the half-life of this antibody in dogs, thereby enhancing its effectiveness for long-term treatment. This modification is crucial for maintaining therapeutic levels of the antibody in the bloodstream, thereby improving overall treatment outcomes.

One limitation of our study is the use of a mouse model for in vivo experiments. Although the NOG mouse model is a valuable system for evaluating antitumor efficacy, it does not fully recapitulate the canine immune system. Therefore, further studies in canine clinical trials are necessary to validate the safety and efficacy of anti-PD-L1 antibodies. Additionally, our study focused on PD-L1 as a target; however, the canine tumor microenvironment is complex and involves multiple immune checkpoints and regulatory pathways. Future research should explore the efficacy of combination therapies that target multiple checkpoints or incorporate other modalities, such as adoptive cell transfer or cancer vaccines, to enhance therapeutic efficacy. Another limitation of canine tumor treatment is the lack of established canine tumor cell lines. Several types of canine tumors exist, among which osteosarcoma and lymphoma are most common. Due to the limited studies on canine tumors, only a few canine cancer cell lines exist. Additionally, treating tumor-bearing canines presents difficulties in recruiting a sufficient number of subjects.

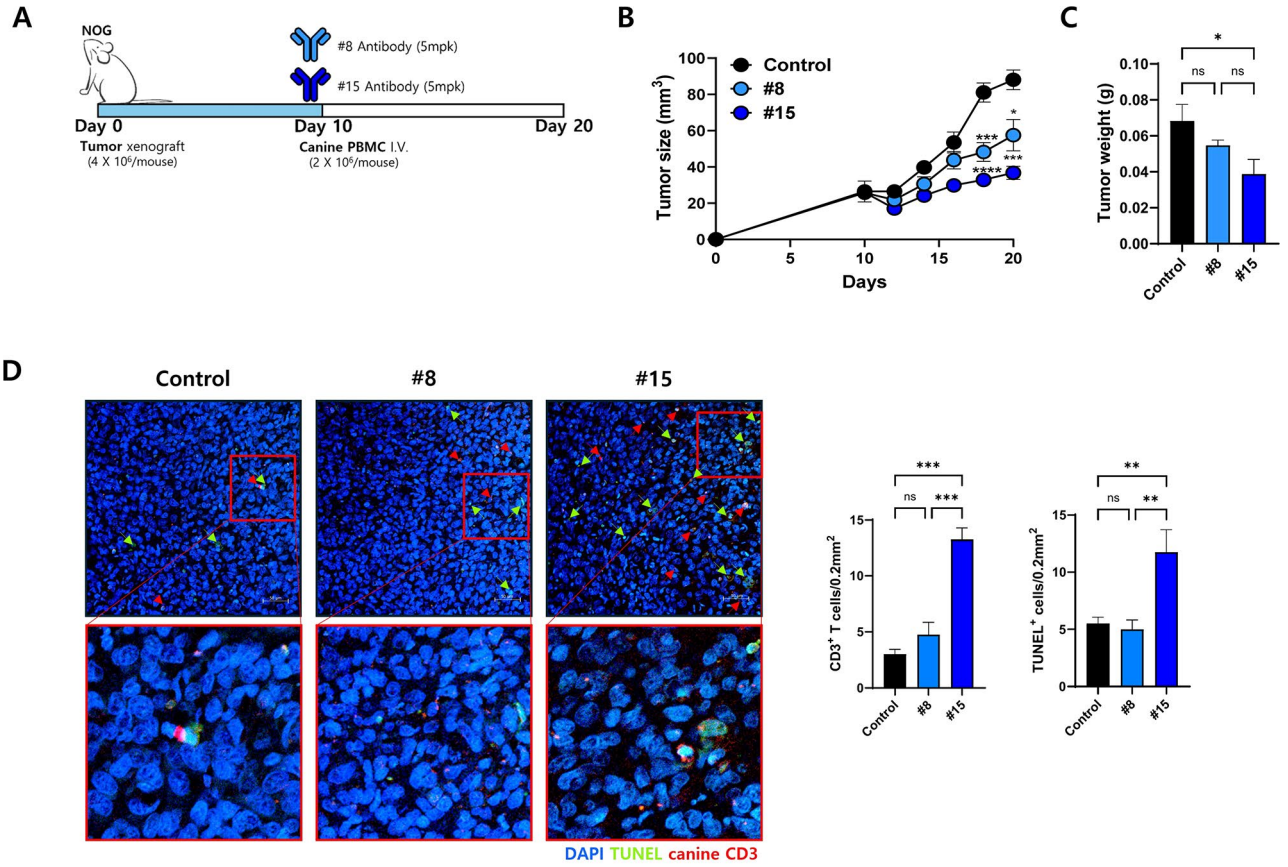

Fig. 5. Antitumor effect of canine PD-L1 antibodies in vivo. (**A**) Schematic representation of the in vivo experiment. (**B**) Groups of mice were grafted with D17 (4×10^6/mouse) into their left flank and monitored for 20 days. Canine PBMC were injected intravenously after 10 days of tumor injection (2×10^6/mouse). #8 or #15 antibody were injected intraperitoneal with the concentration of 1 mg/mL. The tumor growth in mice treated with #8 or #15 antibody. $^{*}p<0.05$, $^{***}p<0.001$, and $^{****}p<0.0001$ (one-way ANOVA; n = 5 per group). (**C**) Tumor mass of mice. ns, not significant and $^{*}p<0.05$ (one-way ANOVA; n = 5 per group). These data are representative of three independent experiments. (**D**) Representative immunofluorescence images of tumors from mice treated with PBMC and canine anti-PD-L1 #8 or #15 antibody. DAPI (blue), TUNEL (green), and canine CD3 (red).

This study represents a significant advancement in developing immunotherapies for canine cancer. The anti-PD-L1 antibodies, particularly #15, show great promise for enhancing the immune response against canine osteosarcoma, potentially leading to improved treatment outcomes. However, continued research and clinical validation will be crucial to bringing these novel therapies to the veterinary field, ultimately improving the quality of life for dogs with cancer and potentially adopting similar strategies for treating human cancer.

Data availability

Further information and requests for resources and reagents should be directed to, and will be fulfilled by, the lead contacts Hyun-Jeong Ko (hjko@kangwon.ac.kr) and Dae Hee Kim (kimdh@kangwon.ac.kr).

Received: 2 September 2024; Accepted: 17 February 2025
Published online: 04 March 2025

References

1. Chibuk, J. et al. Horizons in veterinary precision oncology: Fundamentals of cancer genomics and applications of liquid biopsy for the detection, characterization, and management of cancer in dogs. *Front. Vet. Sci.* **8**, 664718 (2021).
2. Fleming, J. M., Creevy, K. E. & Promislow, D. E. Mortality in North American dogs from 1984 to 2004: An investigation into age-, size-, and breed-related causes of death. *J. Vet. Intern. Med.* **25**, 187–198 (2011).
3. Merlo, D. F. et al. Cancer incidence in pet dogs: Findings of the animal tumor registry of Genoa. *Italy. J. Vet. Intern. Med.* **22**, 976–984 (2008).
4. Rafalko, J. M. et al. Age at cancer diagnosis by breed, weight, sex, and cancer type in a cohort of more than 3,000 dogs: Determining the optimal age to initiate cancer screening in canine patients. *PLOS ONE* **18**, e0280795 (2023).
5. Oh, J. H. & Cho, J. Y. Comparative oncology: Overcoming human cancer through companion animal studies. *Exp. Mol. Med.* **55**, 725–734 (2023).

6. Baioni, E. et al. Estimating canine cancer incidence: Findings from a population-based tumour registry in northwestern Italy. *BMC Vet. Res.* **13**, 203 (2017).
7. Todorova, I. Prevalence and etiology of the most common malignant tumours in dogs and cats. *Bulg. J. Vet. Med.* **9**, 85–98 (2006).
8. Regan, D., Guth, A., Coy, J. & Dow, S. Cancer immunotherapy in veterinary medicine: Current options and new developments. *Vet. J.* **207**, 20–28 (2016).
9. Zahavi, D. & Weiner, L. Monoclonal antibodies in cancer therapy. *Antibodies* **9**, 34 (2020).
10. Lee, H. M. Strategies for manipulating T cells in cancer immunotherapy. *Biomol. Ther. (Seoul)* **30**, 299–308 (2022).
11. Marhelava, K., Pilch, Z., Bajor, M., Graczyk-Jarzynka, A. & Zagozdzon, R. Targeting negative and positive immune checkpoints with monoclonal antibodies in therapy of cancer. *Cancers* **11**, 1756 (2019).
12. Ahn, J. H. et al. A novel anti-PD-L1 antibody exhibits antitumor effects on multiple myeloma in murine models via antibody-dependent cellular cytotoxicity. *Biomol. Ther. (Seoul)* **29**, 166–174 (2021).
13. Ishida, Y., Agata, Y., Shibahara, K. & Honjo, T. Induced expression of PD-1, a novel member of the immunoglobulin gene superfamily, upon programmed cell death. *EMBO J.* **11**, 3887–3895 (1992).
14. Cho, J. et al. Bispecific antibody-bound T cells as a novel anticancer immunotherapy. *Biomol. Ther. (Seoul)* **30**, 418–426 (2022).
15. Cha, J. H., Chan, L. C., Li, C. W., Hsu, J. L. & Hung, M. C. Mechanisms controlling PD-L1 expression in cancer. *Mol. Cell* **76**, 359–370 (2019).
16. Riella, L. V., Paterson, A. M., Sharpe, A. H. & Chandraker, A. Role of the PD-1 pathway in the immune response. *Am. J. Transplant* **12**, 2575–2587 (2012).
17. Jiang, Y., Chen, M., Nie, H. & Yuan, Y. PD-1 and PD-L1 in cancer immunotherapy: Clinical implications and future considerations. *Hum. Vaccin. Immunother.* **15**, 1111–1122 (2019).
18. Qin, S. et al. Novel immune checkpoint targets: Moving beyond PD-1 and CTLA-4. *Mol. Cancer* **18**, 155 (2019).
19. Pardoll, D. M. The blockade of immune checkpoints in cancer immunotherapy. *Nat. Rev. Cancer* **12**, 252–264 (2012).
20. Maekawa, N. et al. PD-L1 immunohistochemistry for canine cancers and clinical benefit of anti-PD-L1 antibody in dogs with pulmonary metastatic oral malignant melanoma. *Npj Precis. Oncol.* **5**, 10 (2021).
21. Maekawa, N. et al. Expression of PD-L1 on canine tumor cells and enhancement of IFN-γ production from tumor-infiltrating cells by PD-L1 blockade. *PLOS ONE* **9**, e98415 (2014).
22. Choi, J. W. et al. Development of canine PD-1/PD-L1 specific monoclonal antibodies and amplification of canine T cell function. *PLOS ONE* **15**, e0235518 (2020).
23. Maekawa, N. et al. A canine chimeric monoclonal antibody targeting PD-L1 and its clinical efficacy in canine oral malignant melanoma or undifferentiated sarcoma. *Sci. Rep.* **7**, 8951 (2017).
24. Tateyama, N. et al. Antitumor activity of an anti-EGFR/HER2 bispecific antibody in a mouse xenograft model of canine osteosarcoma. *Pharmaceutics* **14**, 2494 (2022).
25. Barbas, C. F. *Phage Display: A Laboratory Manual* (Cold Spring Harbor Lab., 2001).
26. Yang, H. Y., Kang, K. J., Chung, J. E. & Shim, H. Construction of a large synthetic human scFv library with six diversified CDRs and high functional diversity. *Mol. Cells* **27**, 225–235 (2009).
27. Lim, H. Investigation of protein-protein interactions and hot spot region between PD-1 and PD-L1 by fragment molecular orbital method. *Sci. Rep.* **9**, 16727 (2019).
28. Hansen, K. & Khanna, C. Spontaneous and genetically engineered animal models; use in preclinical cancer drug development. *Eur. J. Cancer* **40**, 858–880 (2004).
29. Aleyassine, H. & Frei, J. Energetic leukocyte metabolism II Incorporation of phosphate-P32 into leukocytes and identification of p-32 labelled compounds by high voltage electrophoresis. *Enzymol. Biol. Clin. (Basel)* **7**, 89–97 (1966).
30. Khanna, C. et al. The dog as a cancer model. *Nat. Biotechnol.* **24**, 1065–1066 (2006).
31. José-López, R. Chemotherapy for the treatment of intracranial glioma in dogs. *Front. Vet. Sci.* **10**, 1273122 (2023).
32. Nosalova, N. et al. Canine mammary tumors: Classification, biomarkers, traditional and personalized therapies. *Int. J. Mol. Sci.* **25**, 2891 (2024).
33. Jeong, S. & Park, S.-H. Co-stimulatory receptors in cancers and their implications for cancer immunotherapy. *Immune Netw.* **20**, e3 (2020).
34. Maeda, S. Second era of molecular-targeted cancer therapies in dogs. *J. Vet. Med. Sci.* **85**, 790–798 (2023).
35. Giuliano, A., Pimentel, P. A. B. & Horta, R. S. Checkpoint inhibitors in dogs: Are we there yet?. *Cancers* **16**, 2003 (2024).
36. Mason, N. J. et al. Development of a fully canine anti-canine CTLA4 monoclonal antibody for comparative translational research in dogs with spontaneous tumors. *Mabs* **13**, 2004638 (2021).
37. Igase, M. et al. A pilot clinical study of the therapeutic antibody against canine PD-1 for advanced spontaneous cancers in dogs. *Sci. Rep.* **10**, 18311 (2020).
38. Oh, W. et al. Development of an anti-canine PD-L1 antibody and caninized PD-L1 mouse model as translational research tools for the study of immunotherapy in humans. *Cancer Res. Commun.* **3**, 860–873 (2023).
39. Dhawan, D., Hahn, N. M., Ramos-Vara, J. A. & Knapp, D. W. Naturally-occurring canine invasive urothelial carcinoma harbors luminal and basal transcriptional subtypes found in human muscle invasive bladder cancer. *PLOS Genet.* **14**, e1007571 (2018).
40. Kwon, J. Y., Moskwa, N., Kang, W., Fan, T. M. & Lee, C. Canine as a comparative and translational model for human mammary tumor. *J. Breast Cancer* **26**, 1–13 (2023).
41. Gardner, H. L., Fenger, J. M. & London, C. A. Dogs as a model for cancer. *Annu. Rev. Anim. Biosci.* **4**, 199–222 (2016).

Acknowledgements

This research was supported by the National Research Foundation of Korea (NRF) grant funded by the Korean Government (Ministry of Science and ICT, grant number: 20201R1A5A8019180).

Author contributions

Conceptualization: HJK and DHK; Methodology: JC and MYS; Investigation: HP, KK, MYS, and YS; Statistical analysis: HP, AJH and YS; Supervision: JC, LCM and DHK; Writing: JC, MYS, and HJK; Guarantor: HJK and DHK.

Declarations

Competing interests

The authors declare no competing interests.

Additional information

Supplementary Information The online version contains supplementary material available at https://doi.org/1

0.1038/s41598-025-90770-1.

Correspondence and requests for materials should be addressed to D.H.K. or H.-J.K.

Reprints and permissions information is available at www.nature.com/reprints.

Publisher's note Springer Nature remains neutral with regard to jurisdictional claims in published maps and institutional affiliations.

Open Access This article is licensed under a Creative Commons Attribution-NonCommercial-NoDerivatives 4.0 International License, which permits any non-commercial use, sharing, distribution and reproduction in any medium or format, as long as you give appropriate credit to the original author(s) and the source, provide a link to the Creative Commons licence, and indicate if you modified the licensed material. You do not have permission under this licence to share adapted material derived from this article or parts of it. The images or other third party material in this article are included in the article's Creative Commons licence, unless indicated otherwise in a credit line to the material. If material is not included in the article's Creative Commons licence and your intended use is not permitted by statutory regulation or exceeds the permitted use, you will need to obtain permission directly from the copyright holder. To view a copy of this licence, visit http://creativecommons.org/licenses/by-nc-nd/4.0/.

© The Author(s) 2025